

Entanglement in Resonance Fluorescence

Juan Camilo López Carreño,^{1,*} Santiago Bermúdez Feijoo,² and Magdalena Stobińska³

¹*Institute of Theoretical Physics, University of Warsaw, ul. Pasteura 5, 02-093, Warsaw, Poland*

²*Departamento de Física, Universidad Nacional de Colombia, Ciudad Universitaria, K. 45 No. 26–85, Bogotá D.C., Colombia*

³*Faculty of Mathematics, Informatics and Mechanics, University of Warsaw, ul. Banacha 2, 02-097 Warsaw, Poland*
(Dated: June 19, 2023)

Particle entanglement is a fundamental resource upon which are based many quantum technologies. However, the up-to-now best sources of entangled photons rely on parametric down-conversion processes, which are optimal only at certain frequencies, which rarely match the energies of condensed-matter systems that can benefit from entanglement. In this Article, we show a way to circumvent this issue, and we introduce a new source of entangled photons based on resonance fluorescence delivering photon pairs as a superposition of vacuum and the Bell state $|\Phi^-\rangle$. Our proposal relies on the emission from the satellite peaks of a two-level system driven by a strong off-resonant laser, whose intensity controls the frequencies of the entangled photons. Furthermore, the degree of entanglement can be optimized for every pair of frequencies, thus demonstrating a clear advantage over existing technologies. Finally, we illustrate the power of our novel source of entangled single-photon pairs by exciting a system of polaritons and showing that they are left in a maximally entangled steady state.

Resonance fluorescence, the interaction between an artificial atom and coherent light, has been the subject of fundamental research from the early stages of quantum optics.^{1,2} In particular, the observation of photon antibunching from this interaction³ paved the way for investigations regarding the quantum character of light, and the phenomena that has enabled, for instance, the pursue of single-photon transistors.⁴ In turn, single photon emission is a key element for many quantum information technologies,^{5,6} allowing the possibility to design protocols for, e.g., quantum teleportation⁷ and quantum cryptography.⁸ Usually, the source of light is a laser (with a well defined energy) which effectively matches a single energy transition of the artificial atom, and therefore, in practice, one deals with the excitation of a so-called “two-level system” (2LS). Thus, the laser can only induce a single excitation in the atom at the time, and which has led resonance fluorescence to be regarded as an ultrabright source of quantum light,^{5,9,10} with high single-photon purity.^{11,12} However, recent investigations that analysed the luminescence with spectral resolution,¹³ have found that the emission from a 2LS actually consists of multiple highly-correlated photons.^{14–20}

Such a multi-photon structure is particularly revealed when the intensity of the driving laser is strong and the 2LS enters into the so-called *Mollow regime*,²¹ in which the emission spectrum of the 2LS consists of a triplet, as illustrated in dashed lines in Fig. 1(a). Notably, although the photons emitted from the 2LS are perfectly antibunched, selecting particular frequency regions of the emission allows to unveil a richer landscape of photon correlations^{14–16}—ranging from antibunching to superbunching statistics, passing through thermal and uncorrelated light. In fact, the statistical variability of the photons emitted by resonance fluorescence allows to design exotic sources of light,²² excite other optical targets,^{23–25} and perform the so-called *Mollow spectroscopy*,²³ whereby, e.g., the internal structure of complex and highly-dissipative quantum systems can be probed with a minimal amount of photons, namely, two.

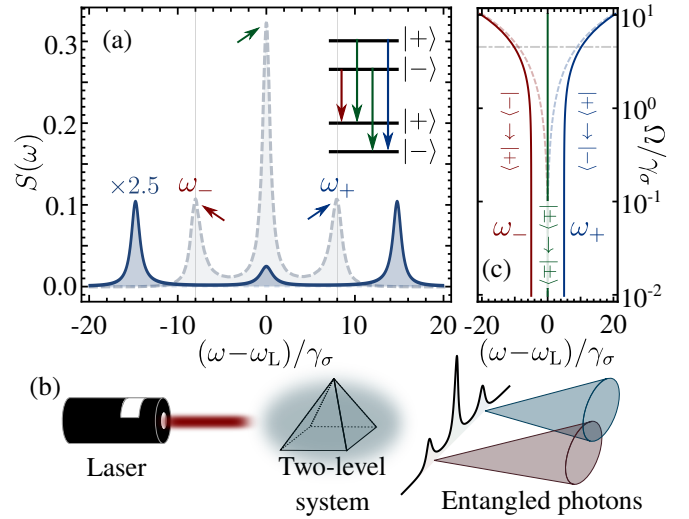


Figure 1. (Color online). The Mollow triplet driven out of resonance. (a) Emission spectrum when the laser is resonant (dashed) and detuned (solid) from the 2LS. The emission lines are identified with the four possible transitions (two of them are degenerate) between the dressed states (shown in the inset). (b) Scheme of our proposed source of entangled photon pairs emitted from the sidebands of the Mollow triplet. (c) Energy transitions enabling the emission from the 2LS as a function of the driving intensity. In the detuned case (solid, dark lines), and as opposed to the resonant one (dashed, light lines), the satellite peaks become the dominant feature of the spectrum, and the dynamics is given by transitions that change the quantum state of the 2LS, i.e., by transitions of the type $|\pm\rangle \rightarrow |\mp\rangle$ (shown in red and blue). For the figure we used γ_σ as the unit, $\Omega/\gamma_\sigma = 4$ (marked in panel (c) as a horizontal gray line) and $(\omega_\sigma - \omega_L)/\gamma_\sigma = 25/2$.

In this Article, we approach a different type of quantum correlations, namely entanglement, which has been observed in Resonance Fluorescence when either a collection of atoms is considered²⁶ or its biexciton structure is taken into account²⁷ and the 2LS is coupled to a microcavity.^{9,28–32} Here, we demonstrate that time-frequency entanglement can be ex-

tracted from resonance fluorescence, specifically, from the emission of a Mollow triplet, without the need of coupling it to other objects or taking into account any additionally internal structures of the 2LS. Instead, one only needs to include the observation of the emission into the description. In fact, we show that when the 2LS is driven out of resonance, the emission from the sidebands of the triplet behave as a heralded source of entangled photon pairs, as sketched in Fig. 1(b).

An important advantage that our proposal has over existing technologies, e.g., sources based on parametric downconversion processes is that the entangled photons pairs emitted by our source follow an antibunched (and not an uncorrelated) statistics. Thus, while in sources based on SPDC a higher intensity of driving produces higher-order processes, our source produces more pairs of entangled photons. Finally, noting that the Mollow regime has been successfully realized in a variety of systems, including quantum dots,^{33–38} molecules,³⁹ cold atom ensembles,⁴⁰ confined single atoms,⁴¹ photonic chips,⁴² and superconducting qubits^{43–45} (and 2LSs can also be constructed in other platforms including superconducting circuits^{46–52} and photonic structures^{53–55}), our source is able to operate on a wide gamut of frequencies and to interface with, e.g., condensed-matter systems that can benefit from entangled excitation,⁵⁶ thus making resonance fluorescence a compelling alternative to the existing sources of entangled photons.

The rest of this Article is organized as follows: We first demonstrate that energy-time entangled between photons emitted from the sidebands of the 2LS is unveiled simply by including the observation of the light into the description of our system. Next, we use a quantum Monte Carlo experiment to demonstrate that, as a consequence of the detuned excitation, the entangled photon pairs are heralded. Finally, we show that our source is able to drive complex condensed-matter systems (e.g., exciton-polaritons⁵⁷) into a maximally entangled steady state, despite them being immersed within a highly-dissipative environment.

RESULTS

Measurement of the photons

A key aspect of quantum mechanics is that measurements affect the quantum state of the system under observation. Thus, a correct description of the emission from the 2LS should also incorporate in the dynamics the effect of the observation by a physical detector, namely one able to observe photons of a given frequency $\tilde{\omega}$ with a finite linewidth $\tilde{\Gamma}$. Such a description can be done with the theory of frequency-resolved correlations,¹³ whereby detectors are considered as quantum mechanical objects that receive the excitation from the source of light without returning any feedback. In practice, this can be achieved by coupling the emitter and the detectors with a vanishing strength,¹³ or by using the formalism of *cascaded systems*.^{58,59} While these two approaches yield exactly the same normalized correlations (i.e., n^{th} -order

correlation functions),⁶⁰ the latter also provides the correct un-normalized correlations (e.g., the mean population or the emission rate of the system), and therefore it is the implementation that we will use throughout this Article. Using the master equation outlined in the Methods section, we gain access to the correlations between photons from the Mollow triplet emitted at frequencies ω_1 and ω_2 . In particular, we are interested in the second-order correlation between photons emitted at the frequencies of the satellite peaks (with energies ω_{\pm} , c.f. the scheme in Fig. 1, associated to bosonic annihilation operator a_1 and a_2) separated by a time τ , i.e., we compute $g_{12}^{(2)}(\tau) = \langle a_1^\dagger a_2^\dagger(\tau) a_2(\tau) a_1 \rangle / (\langle a_1^\dagger a_1 \rangle \langle a_2^\dagger a_2 \rangle)$ for the case where $\omega_1 = \omega_+$ and $\omega_2 = \omega_-$. Note that while the inclusion of detection into the description of the emission leads to a loss of antibunching of the signal,⁶¹ it also unveils the multi-photon structure behind the dynamics of the 2LS.¹⁶

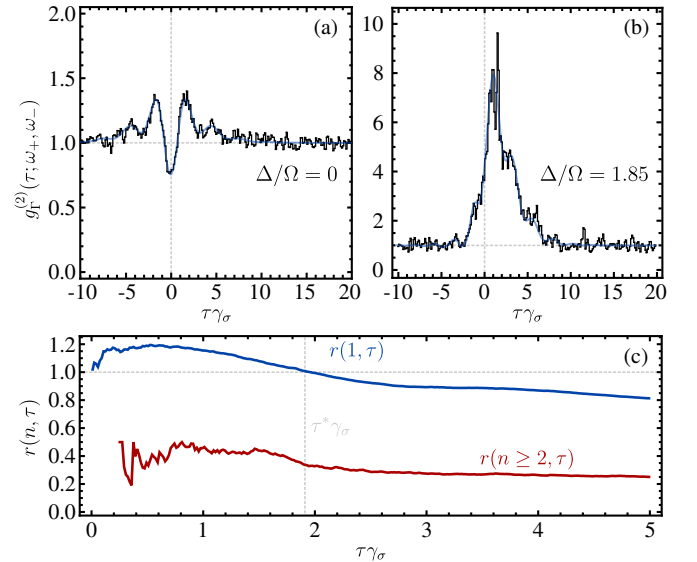


Figure 2. (Color online). Herald single photons observed through a frequency-resolved quantum Monte Carlo experiment. (a, b) Crossed-correlations between photons detected with frequencies ω_+ and ω_- , showing the agreement with theoretical prediction (solid blue lines) and the quantum Monte Carlo experiment (black bars). When the driving laser is resonant to the 2LS, the correlation function is completely symmetric (cf. panel a). When the driving is taken out of resonance, the shape of the correlation function resembles a λ , indicating that the emission of a photon with frequency ω_+ heralds the emission of a photon with frequency ω_- (cf. panel b). (c) Ratio $r(n, \tau) = p(n, \tau, \Delta)/p(n, \tau, 0)$ of the probability to detect one (blue) and two or more (red) photons after detecting the heralding photon, when the driving is made out of resonance and in resonance. Taking the laser out of resonance enhances the single-photon heralding probability within a time-window τ^* of almost two lifetimes of the 2LS, as indicated by the dashed vertical line. Additionally, the probability to herald two or more photons is suppressed when the driving is done out of resonance. For the figures we used γ_σ as the unit, and the parameters that optimize entangled emission from the sidebands of the triplet (cf. Section II of the Supplemental Material); namely $\Omega/\gamma_\sigma = 1$, $\Gamma/\gamma_\sigma = 1$, and $\Delta = 1.85\Omega$.

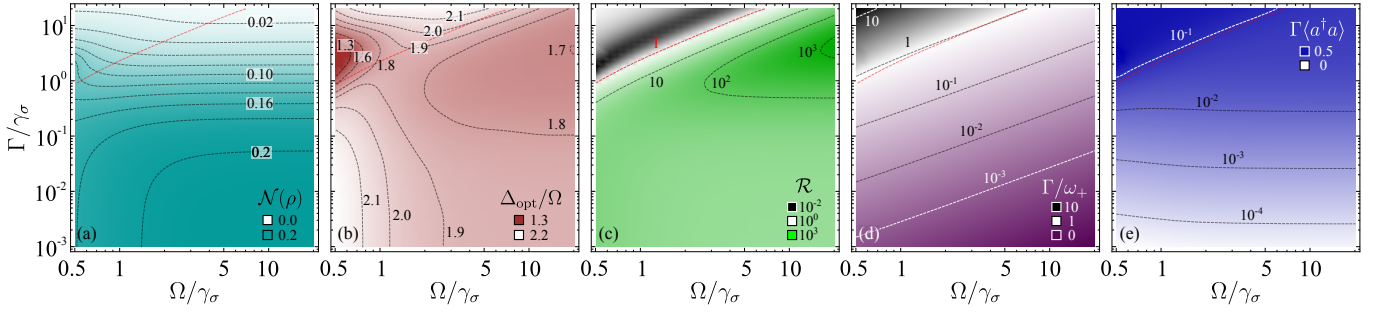


Figure 3. (Color online). Characterisation of our source of entangled pairs of single photons. (a) Maximum logarithmic negativity that can be reached as a function of the linewidth of the detectors and the intensity of the driving laser, which indicates that the optimal condition for extracting entanglement is to have narrow detectors observing a Mollow triplet with a very large splitting (namely, the bottom right corner of the panel). (b) The optimum detuning at which the 2LS must be driven depends both on the intensity of the driving and the linewidth of the detectors or, equivalently, the optimal targets receiving the entangled photons. (c) Violation of the CSI showing the regions where the negativity obtained in panel (a) is not an artifact of the competition between the detectors for the photons of the sidebands. (d) The ratio between the linewidth of the detectors and the splitting between the sidebands. It shows that the best configurations are those for which this ratio is as small as possible, and that it has to be less than 1 to violate the CSI. (e) Emission rate from the detectors, thus completing the mapping of the quality and the brightness of the source of entangled single photons based on the Mollow triplet. The red, diagonal, dotted line on each panel indicates the boundary above which the emission does not violate the CSI.

When the latter is driven resonantly by a laser, its $g_{12}^{(2)}(\tau)$ is completely symmetric, as shown in Fig. 2(a). Such a shape is an indication that the emission from the high-energy sideband (with frequency ω_+) can occur either before or after the emission from the low-energy peak (with frequency ω_-); i.e., there is not a causal relation between consecutive emissions. Such a symmetry is broken when the driving laser (with frequency ω_L) is taken out of resonance from the 2LS (with natural frequency ω_σ). Figure 2(b) shows the case for $\Delta \equiv (\omega_\sigma - \omega_L) = 1.85\Omega$, where it is clear that the emission from the high-energy sideband occurs *after* the emission of a photon from the low-energy one (the reverse situation occurs if the detuning becomes negative). While the type of correlation shown in Fig. 2(b) is indicative of a heralded emission, it does not necessarily imply that the emission consists of single photons. To show that this is in fact the case, we performed a frequency-resolved quantum Monte Carlo simulation⁶⁰ of the emission from the two sidebands of the Mollow triplet to compare the cases when the 2LS is driven in and out of resonance. Thus, from the simulations we are able to obtain the probability $p(n, \tau, \Delta)$ to detect n photons of energy ω_+ within a time-window τ after a photon of energy ω_- has been measured, provided that the detuning between the 2LS and the laser is Δ . Figure 2(c) shows the ratios $r(n, \tau) = p(n, \tau, \Delta)/p(n, \tau, 0)$, which illustrate that the detuning enhances the probability to detect one photon by about 20% (blue line) while simultaneously decreases the probability to detect two or more photons (red line). Note that the ratio $r(1, \tau)$ becomes less than one for time windows larger than $\tau^* \approx 2/\gamma_\sigma$, shown as a vertical dashed line in Fig. 2(c). Thus, the heralded photons are more likely to be emitted within the time window $\tau \leq \tau^*$ when the 2LS is driven out of resonance. Together, Fig. 2(b) and (c) are the evidence that demonstrates that a 2LS driven out of resonance by a laser is a source of heralded single photons, whose frequencies

correspond to the energies of the sidebands of the Mollow triplet.

Source of entangled photon pairs

Now that we have established that the emission from the satellite peaks of the detuned Mollow triplet is composed of highly correlated pairs of single photons, and that their emission can be observed in a heralded fashion, we investigate another type of quantum correlation: entanglement. It has been theoretically predicted¹⁷ and experimentally observed¹⁵ that pairs of photons emitted from the Mollow spectrum at various frequencies violate the Cauchy-Schwarz inequality (CSI), which can only happen in systems displaying entanglement.⁶² Thus, in our Article we quantify entanglement through the so-called *logarithmic negativity* $\mathcal{N}(\rho)$,^{63–65} which is an entanglement monotone⁶⁶ that quantifies the degree to which the partial transposition of the quantum state violates the criterion of positivity.⁶⁷

Independently of the detuning between the 2LS and the laser that takes it into the Mollow regime, there are always pairs of frequencies $\tilde{\omega}_1$ and $\tilde{\omega}_2$ for which the CSI is violated.¹⁷ However, although the latter is an indication of entanglement, the logarithmic negativity only becomes nonzero when the laser is taken out of resonance from the 2LS. Figure 3(a) shows the maximum $\mathcal{N}(\rho)$ that can be extracted from photons emitted at the sidebands, depending on both the intensity of the driving Ω and the linewidth of the detector Γ . Here, each point is obtained for the optimum detuning Δ_{opt} between the laser and the 2LS, which we display in Fig. 3(b). For the largest part of the figure, the detuning that optimizes the entanglement is around $\Delta \sim 2\Omega$. However, in the upper left corner of the panel we find a region for which the optimal condition is found near resonance. However, looking at the map of the CSI violation, shown in in Fig. 3(c), we find that such a region is compatible with a classical state, as the ratio R falls below one (cf. Sec. II

of the Supplemental Material). For visual aid, we have added the $R = 1$ contour as a red dashed line in all the panels. Note that the behaviour of the CSI, together with the artificial disruption in the logarithmic negativity, is a consequence of the competition of the detectors for photons emitted from the two sidebands, as quantified by the ratio Γ/ω_+ , which we show in Fig. 3(d): the CSI violation starts precisely when this ratio becomes strictly less than one, and the photons emitted from the lateral peaks become distinguishable in frequency. Finally, in Figure 3(e) we show the emission rate of the detectors, i.e., $I = \Gamma\langle a^\dagger a \rangle$, as a function of the intensity of the laser and the linewidth of the detectors (the detuning between the 2LS and the laser is taken as in panel (b)), thus making evident the interplay between the quantity and the quality of the signal: the highest degree of entanglement is found when the peaks are very well separated from each other (i.e., $\Omega/\gamma_\sigma \gg 1$) and the linewidth of the observer is narrow (with Γ/γ_σ as small as possible), which in turn comes with the price that such a narrow linewidth decreases the emission rate of the source. In fact, in the configurations realized in the bottom right corner of the panels of Fig. 3, the quantum state of the pairs of entangled single photons is described—with a 97% fidelity—as the superposition of the vacuum and the state $\tilde{\rho} \equiv |\Phi^-\rangle\langle\Phi^-|$. The latter is given by the Bell state

$$|\Phi^-\rangle = \frac{1}{\sqrt{2}}(|0,0\rangle - |1,1\rangle), \quad (1)$$

with a purity of 91.6%, and its contribution to the full quantum state ranges from 0 to 0.6%. Such a small contribution indicates that, although the photons are maximally entangled, one needs to wait for them to be emitted, as discussed above. Furthermore, we find that entanglement is spoiled as the linewidth of the detectors becomes large as compared to the emission lines of the triplet. This is because wide detectors effectively erase the spectral information of the photons, and the emission from the sidebands becomes indistinguishable. However, one can overcome such an issue by driving the 2LS deeper into the Mollow regime, i.e., increasing the intensity of the laser, and thus taking the satellite peaks further away from each other. Notably, the pair of parameters (Ω, Δ) that optimize the logarithmic negativity between the photons from the sidebands of the triplet do not optimize the violation of the CSI nor maximize their second-order correlation function (cf. Section II of the Supplemental Material).

Entangling polaritons

A direct application of the results presented in the previous section is the excitation of one of the most ubiquitous systems in condensed matter physics; namely a pair of coupled bosonic fields. While the latter can represent a large variety of quantum systems, in the following we will associate them to the so-called exciton-polaritons (henceforth, simply *polaritons*); which are pseudo-particles arising from the strong coupling between a photon and an exciton, either within a semiconductor microcavity⁵⁷ or on an organic sample.^{68,69} The dynamics of polaritons driven by resonance fluorescence is given by the

master equation outlined in the Methods section, and we assume that the polaritons are in the strong coupling regime, in which the energy states become dressed and the light emitted is observed at the frequencies of the lower- and upper-polariton branches (cf. the full derivation in Sec. III of the Supplemental Material). Figure 4(a) shows the concurrence between the polariton branches after the vacuum contribution has been removed through a post-selection process. We find that for entanglement to be observed it is necessary that: *i*) the photonic decay rate has to be at least an order of magnitude larger than the rate at which the source is emitting light (we find that, i.e., $\Gamma_a/\gamma_\sigma \approx 30$ is typically enough) and *ii*) the polariton light-matter coupling should be of the order of magnitude of the decay of our source. The first condition guarantees that there are at most two polaritons in the system at any given time, whereas the latter prevents the excitations to be localized in a single polariton branch, thus preserving entanglement. The polariton quantum state that yields the maximum concurrence is shown in Fig. 4(b) before and in Fig. 4(c) after a post-selection process removing the vacuum contribution. Here, we find that the quantum state of the polaritons has a 0.997 fidelity with a superposition between vacuum and the Bell state $|\Psi^-\rangle = \frac{1}{\sqrt{2}}(|0,1\rangle - |1,0\rangle)$, where we have used the notation $|m,n\rangle$ to label a Fock state of polaritons with m and n particles in the lower and upper branch, respectively. These remarkable results show the power of our source of entangled photons, while providing further evidence supporting the observation that polaritons sustain entanglement,⁵⁶ which makes them an attractive platform to perform, e.g., quantum communication and cryptography. These applications, how-

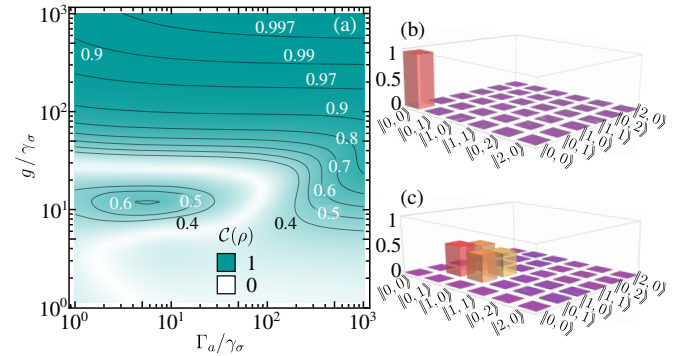


Figure 4. (Color online). Maximally entangled polaritons. (a) Concurrence between the lower- and the upper-polariton branches, reaching up to 91%. (b) Quantum state tomography of the quantum state of polaritons. (c) Same as panel (b) after a post-selection process removing the vacuum. The remaining quantum state has a 0.997 fidelity with a superposition of vacuum and the Bell state $|\Psi^-\rangle$. The figure has been done using the parameters that optimize the entanglement of the photons emitted by the source, namely $\Omega/\gamma_\sigma = 4.9$, $\Delta/\gamma_\sigma = 8.92$ and letting the photon and the exciton be in resonance with the higher- and lower-energy sideband of the triplet, respectively. For panels (b) and (c) we have also used the parameters that yield the maximum concurrence between the polaritons, i.e., $\Gamma_a/\gamma_\sigma = 10$, $g/\gamma_\sigma \approx 300$ and $\Gamma_b \ll \Gamma_a$.

ever, lay outside the scope of this Article and will be left for future research.

DISCUSSION AND CONCLUSIONS

We have described a novel source of entangled photon pairs, based on the Mollow triplet regime of resonance fluorescence. In fact, we showed that when the laser driving the two-level system (2LS) becomes detuned from the natural frequency of the 2LS, the lateral peaks of the triplet become the dominant feature of the emission spectrum. Thus, using the theory of frequency resolved correlations¹³ we showed that, when one focuses on the photons emitted from such lateral peaks, one finds that their emission is heralded. Considering the dressed-atom picture, we showed that these photons, emitted at frequencies ω_+ and ω_- (cf. the scheme in Fig. 1), are the result of two atomic transitions that change the quantum state of the 2LS, and therefore cannot take place twice in a row. Instead, they alternate in such a way that the emission of a photon ω_+ favours the emission of a photon ω_- (note that the opposite order can be achieved if the laser is blue- instead of red-shifted with respect to the 2LS). We have used a quantum Monte Carlo experiment to show that, taking the laser out of resonance from the 2LS, not only leads to the heralding behaviour, but also suppresses emissions consisting of more than one photons; namely, our system operates as a source of heralded single photons.

Analysing the quantum correlations between the single photons emitted from the lateral peaks of the detuned Mollow triplet, we find that they are emitted in a superposition of vacuum and the Bell state $|\Phi^-\rangle$. Furthermore, we have obtained the volume in the parameter space for which the photons violate the Cauchy-Schwarz inequality. Thus, we observe that for the photons to display quantum energy-time entanglement, the linewidth of the detector—or, more generally, the optical target of the emission—has to be narrower than the separation between the lateral peaks of the triplet. Otherwise, the degree of indistinguishability of the photons emitted from the two peaks decreases, which in turn leads to the loss of entanglement. Furthermore, we showed the relation between the emission rate of our source and the degree of entanglement, as measured through the logarithmic negativity. Thus, our manuscript can be used as a road map for the experimental implementation of a source of entangled photons based on resonance fluorescence.

Lastly, to demonstrate the power of our source, we used it to excite an ubiquitous quantum system, commonly recurring in condensed-matter physics, namely a pair of coupled harmonic oscillators embedded in a dissipative environment. Thus, we use the example of exciton-polaritons (although our results are also applicable to systems composed or containing phonons, plasmons, bosonic nanoparticles, and photonics in general) and showed that our source is capable to inject entangled particles into the polariton system, and that, in turn, they are able to maintain such quantum correlations in spite of the decoherence introduced by spontaneous decay. We note

that our model for polaritons has already been used to explain experimental results,⁵⁶ and while further elements of decoherence may be relevant in the analysis of the entanglement in polaritons, their consideration would take us far away the scope of the present paper and therefore are left for future references.

* juclopezca@gmail.com

- [1] H. J. Kimble and L. Mandel, Theory of Resonance Fluorescence, *Phys. Rev. A* **13**, 2123 (1976).
- [2] L. Allen and J. H. Eberly, *Optical Resonance and Two-Level Atoms* (Dover, 1987).
- [3] H. J. Kimble, M. Dagenais, and L. Mandel, Photon Antibunching in Resonance Fluorescence, *Phys. Rev. Lett.* **39**, 691 (1977).
- [4] D. E. Chang, A. S. Sørensen, E. A. Demler, and M. Lukin, A Single-Photon Transistor Using Nanoscale Optical Transistor, *Nat. Phys.* **3**, 76 (2007).
- [5] P. Senellart, G. Solomon, and A. White, High-Performance Semiconductor Quantum-Dot Single-Photon Sources, *Nat. Nanotech.* **12**, 1026 (2017).
- [6] U. Sinha, S. N. Sahoo, A. Singh, K. Joarder, R. Chatterjee, and S. Chakraborti, Single-Photon Sources, *Optics & Photonics News* **30**, 32 (2019).
- [7] D. Fattal, E. Diamanti, K. Inoue, and Y. Yamamoto, Quantum Teleportation with a Quantum Dot Single Photon Source, *Phys. Rev. Lett.* **92**, 037904 (2004).
- [8] A. Beveratos, R. Brouri, T. Gacoin, A. Villing, J.-P. Poizat, and P. Grangier, Single Photon Quantum Cryptography, *Phys. Rev. Lett.* **89**, 187901 (2002).
- [9] A. Dousse, J. Suffczyński, A. Beveratos, O. Krebs, A. Lemaître, I. Sagnes, J. Bloch, P. Voisin, and P. Senellart, Ultrabright Source of Entangled Photon Pairs, *Nature* **466**, 217 (2010).
- [10] O. Gazzano, M. de Vasconcellos, C. Arnold, A. Nowak, E. Galopin, I. Sagnes, L. Lanco, A. Lemaître, and P. Senellart, Bright Solid-State Sources of Indistinguishable Single Photons, *Nat. Comm.* **4**, 1425 (2012).
- [11] J. C. Loredó, N. A. Zakaria, N. Somaschi, C. Anton, L. D. Santis, V. Giesz, T. Grange, M. A. Broome, O. Gazzano, G. Coppola, I. Sagnes, A. Lemaître, A. Auffèves, P. Senellart, M. P. Almeida, and A. G. White, Scalable Performance in Solid-State Single-Photon Sources, *Optica* **3**, 433 (2016).
- [12] N. Somaschi, V. Giesz, L. D. Santis, J. C. Loredó, M. P. Almeida, G. Hornecker, S. L. Portalupi, T. Grange, C. Antón, J. Demory, C. Gómez, I. Sagnes, N. D. Lanzillotti-Kimura, A. Lemaître, A. Auffèves, A. G. White, L. Lanco, and P. Senellart, Near-Optimal Single-Photon Sources in the Solid State, *Nat. Photon.* **10**, 340 (2016).
- [13] E. del Valle, A. González-Tudela, F. P. Laussy, C. Tejedor, and M. J. Hartmann, Theory of Frequency-Filtered and Time-Resolved N-Photon Correlations, *Phys. Rev. Lett.* **109**, 183601 (2012).
- [14] A. González-Tudela, F. P. Laussy, C. Tejedor, M. J. Hartmann, and E. del Valle, Two-Photon Spectra of Quantum Emitters, *New J. Phys.* **15**, 033036 (2013).
- [15] M. Peiris, B. Petrak, K. Konthasinghe, Y. Yu, Z. C. Niu, and A. Muller, Two-Color Photon Correlations of the Light Scattered by a Quantum Dot, *Phys. Rev. B* **91**, 195125 (2015).
- [16] J. C. López Carreño, E. del Valle, and F. P. Laussy, Photon Correlations from the Mollow Triplet, *Laser Photon. Rev.* **11**, 1700090 (2017).
- [17] C. Sánchez Muñoz, E. del Valle, C. Tejedor, and F. P. Laussy,

- Violation of Classical Inequalities by Photon Frequency Filtering, *Phys. Rev. A* **90**, 052111 (2014).
- [18] G. Díaz-Camacho, E. Zubizarreta Casalegua, J. C. López Carreño, S. Khalid, C. Tejedor, E. del Valle, and F. P. Laussy, Multiphoton Emission [10.48550/ARXIV.2109.12049](#) (2021).
- [19] E. Z. Zubizarreta Casalegua, E. del Valle, and F. P. Laussy, Two-photon emission in detuned resonance fluorescence [10.48550/ARXIV.2210.03733](#) (2022).
- [20] L. Masters, X. Hu, M. Cordier, G. Maron, L. Pache, A. Rauschenbeutel, M. Schemmer, and J. Volz, Will a single two-level atom simultaneously scatter two photons? [10.48550/ARXIV.2209.02547](#) (2022).
- [21] B. R. Mollow, Power Spectrum of Light Scattered by Two-Level Systems, *Phys. Rev.* **188**, 1969 (1969).
- [22] C. Sánchez Muñoz, E. del Valle, A. González-Tudela, K. Müller, S. Lichtmanecker, M. Kaniber, C. Tejedor, J. J. Finley, and F. P. Laussy, Emitters of N-photon bundles, *Nature Photon* **8**, 550 (2014).
- [23] J. C. López Carreño, C. Sánchez Muñoz, D. Sanvitto, E. del Valle, and F. P. Laussy, Exciting Polaritons with Quantum Light, *Phys. Rev. Lett.* **115**, 196402 (2015).
- [24] J. C. López Carreño and F. P. Laussy, Excitation with Quantum Light. I. Exciting a Harmonic Oscillator, *Phys. Rev. A* **94**, 063825 (2016).
- [25] J. C. López Carreño, C. Sánchez Muñoz, E. del Valle, and F. P. Laussy, Excitation with Quantum Light. II. Exciting a Two-Level System, *Phys. Rev. A* **94**, 063826 (2016).
- [26] P. Grünwald and W. Vogel, Entanglement in Atomic Resonance Fluorescence, *Phys. Rev. Lett.* **104**, 233602 (2010).
- [27] E. del Valle, Distilling One, Two and Entangled Pairs of Photons from a Quantum Dot with Cavity QED Effects and Spectral Filtering, *New J. Phys.* **15**, 025019 (2013).
- [28] N. Akopian, N. H. Lindner, E. Poem, Y. Berlatzky, J. Avron, D. Gershoni, B. D. Gerardot, and P. M. Petroff, Entangled Photon Pairs from Semiconductor Quantum Dots, *Phys. Rev. Lett.* **96**, 130501 (2006).
- [29] R. M. Stevenson, R. J. Young, P. Atkinson, K. Cooper, D. A. Ritchie, and A. J. Shields, A Semiconductor Source of Triggered Entangled Photon Pairs, *Nature* **439**, 179 (2006).
- [30] S. Schumacher, J. Förstner, A. Zrenner, M. Florian, C. Gies, P. Gartner, and F. Jahnke, Cavity-Assisted Emission of Polarization-Entangled Photons from Biexcitons in Quantum Dots with Fine-Structure Splitting, *Opt. Express* **20**, 5335 (2012).
- [31] R. John, N. A. Gippius, G. Pavlovic, D. D. Solnyshkov, I. A. Shelykh, and G. Malpuech, Entangled Photon Pairs Produced by a Quantum Dot Strongly Coupled to a Microcavity, *Phys. Rev. Lett.* **100**, 240404 (2008).
- [32] P. K. Pathak and S. Hughes, Generation of Entangled Photon Pairs from a Single Quantum Dot Embedded in a Planar Photonic-Crystal Cavity, *Phys. Rev. B* **79**, 205416 (2009).
- [33] K. Konthasinghe, J. Walker, M. Peiris, C. K. Shih, Y. Yu, M. F. Li, J. F. He, L. J. Wang, H. Q. Ni, Z. C. Niu, and A. Muller, Coherent versus Incoherent Light Scattering from a Quantum Dot, *Phys. Rev. B* [10.1103/PhysRevB.85.235315](#) (2012).
- [34] A. Ulhaq, S. Weiler, S. M. Ulrich, R. Roßbach, M. Jetter, and P. Michler, Cascaded Single-Photon Emission from the Mollow Triplet Sidebands of a Quantum Dot, *Nat. Photon.* **6**, 238 (2012).
- [35] A. Muller, E. B. Flagg, P. Bianucci, X. Y. Wang, D. G. Deppe, W. Ma, J. Zhang, G. J. Salamo, M. Xiao, and C. K. Shih, Resonance Fluorescence from a Coherently Driven Semiconductor Quantum Dot in a Cavity, *Phys. Rev. Lett.* **99**, 187402 (2007).
- [36] A. N. Vamivakas, Y. Zhao, C.-Y. Lu, and M. Atatüre, Spin-resolved quantum-dot resonance fluorescence, *Nat. Phys.* **5**, 198 (2009).
- [37] E. B. Flagg, A. Muller, J. W. Robertson, S. Founta, D. G. Deppe, M. Xiao, W. Ma, G. J. Salamo, and C. K. Shih, Resonantly Driven Coherent Oscillations in a Solid-State Quantum Emitter, *Nat. Phys.* **5**, 203 (2009).
- [38] S. Ates, S. M. Ulrich, S. Reitzenstein, A. Löffler, A. Forchel, and P. Michler, Post-Selected Indistinguishable Photons from the Resonance Fluorescence of a Single Quantum Dot in a Microcavity, *Phys. Rev. Lett.* **103**, 167402 (2009).
- [39] G. Wrigge, I. Gerhardt, J. Hwang, G. Zumofen, and V. Sandoghdar, Efficient Coupling of Photons to a Single Molecule and the Observation of Its Resonance Fluorescence, *Nat. Phys.* **4**, 60 (2008).
- [40] L. Ortiz-Gutiérrez, R. C. Teixeira, A. Eloy, D. Ferreira da Silva, R. Kaiser, R. Bachelard, and M. Fouché, Mollow triplet in cold atoms, *New J. Phys.* **21**, 093019 (2019).
- [41] B. L. Ng, C. H. Chow, and C. Kurtsiefer, Observation of the Mollow triplet from an optically confined single atom, *Phys. Rev. A* **106**, 063719 (2022).
- [42] C. Cui, L. Zhang, and L. Fan, Photonic analog of Mollow triplet with on-chip photon-pair generation in dressed modes, *Opt. Lett.* **46**, 4753 (2021).
- [43] O. Astafiev, A. M. Zagoskin, A. A. A. Jr, Y. A. Pashkin, T. Yamamoto, K. Inomata, Y. Nakamura, and J. S. Tsai, Resonance Fluorescence of a Single Artificial Atom, *Science* **327**, 840 (2010).
- [44] A. F. van Loo, A. Fedorov, K. Lalumière, B. C. Sanders, A. Blais, and A. Wallraff, Photon-Mediated Interactions Between Distant Artificial Atoms, *Science* **342**, 1494 (2013).
- [45] D. M. Toyli, A. W. Eddins, S. Boutin, S. Puri, D. Hover, V. Bolkhovskiy, W. D. Oliver, A. Blais, and I. Siddiqi, Resonance Fluorescence from an Artificial Atom in Squeezed Vacuum, *Phys. Rev. X* **6**, 031004 (2016).
- [46] V. Bouchiat, D. Vion, P. Joyez, D. Esteve, and M. H. Devoret, Quantum Coherence with a Single Copper Pair, *Phys. Scr.* **1998**, 165 (1998).
- [47] Y. Nakamura, Y. A. Pashkin, and J. S. Tsai, Coherent Control of Macroscopic Quantum States in a Single-Cooper-Pair Box, *Nature* **398**, 786 (1999).
- [48] J. E. Mooji, T. P. Orlando, L. Levitov, L. Tian, H. van der Wal, and S. Lloyd, Josephson Persistent-Current Qubit, *Science* **285**, 1036 (1999).
- [49] D. Vion, A. Aassime, A. Cottet, P. Joyez, H. Pothier, C. Urbina, D. Esteve, and M. H. Devoret, Manipulating the Quantum State of an Electrical Circuit, *Science* **296**, 886 (2002).
- [50] J. M. Martinis, S. Nam, J. Aumentado, and C. Urbina, Rabi Oscillations in a Large Josephson-Junction Qubit, *Phys. Rev. Lett.* **89**, 117901 (2002).
- [51] J. Koch, T. M. Yu, J. M. Gambetta, A. A. Houck, D. I. Schuster, J. Majer, A. Blais, M. H. Devoret, S. M. Girvin, and R. J. Schoelkopf, Charge-insensitive qubit design derived from the Cooper pair box, *Phys. Rev. A* **76**, 042319 (2007).
- [52] J. A. Schreier, A. A. Houck, J. Koch, D. I. Schuster, B. R. Johnson, J. M. Chow, J. M. Gambetta, J. Majer, L. Frunzio, M. H. Devoret, S. M. Girvin, and R. J. Schoelkopf, Suppressing charge noise decoherence in superconducting charge qubits, *Phys. Rev. B* **77**, 180502 (2008).
- [53] L. Bányai and S. W. Koch, *Semiconductor Quantum Dots*, World Scientific Series on Atomic, Molecular, and Optical Physics No. vol. 2 (World Scientific, Singapore ; River Edge, NJ, 1993).
- [54] J. L. O'Brien, A. Furusawa, and J. Vučković, Photonic Quantum Technologies, *Nat. Phys.* **3**, 687 (2009).
- [55] P. Lodahl, S. Mahmoodian, and S. Stobbe, Interfacing Single Photons and Single Quantum Dots with Photonic Nanostructures,

- Rev. Mod. Phys.* **87**, 347 (2015).
- [56] Á. Cuevas, J. C. López Carreño, B. Silva, M. D. Giorgi, D. G. Suárez-Forero, C. Sánchez Muñoz, A. Fieramosca, F. Cardano, L. Marrucci, V. Tasco, G. Biasiol, E. del Valle, L. Dominici, D. Ballarini, G. Gigli, P. Mataloni, F. P. Laussy, F. Sciarrino, and D. Sanvitto, First Observation of the Quantized Exciton-Polariton Field and Effect of Interactions on a Single Polariton, *Sci. Adv.* **4**, eaao6814 (2018).
 - [57] C. Weisbuch, M. Nishioka, A. Ishikawa, and Y. Arakawa, Observation of the Coupled Exciton-Photon Mode Splitting in a Semiconductor Quantum Microcavity, *Phys. Rev. Lett.* **69**, 3314 (1992).
 - [58] C. W. Gardiner, Driving a Quantum System with the Output Field from Another Driven Quantum System, *Phys. Rev. Lett.* **70**, 2269 (1993).
 - [59] H. J. Carmichael, Quantum Trajectory Theory for Cascaded Open Systems, *Phys. Rev. Lett.* **70**, 2273 (1993).
 - [60] J. C. López Carreño, E. del Valle, and F. P. Laussy, Frequency-Resolved Monte Carlo, *Sci. Rep.* **8**, 6975 (2018).
 - [61] J. C. López Carreño, E. Zubizarreta Casalengua, B. Silva, E. del Valle, and F. P. Laussy, Loss of antibunching, *Phys. Rev. A* **105**, 023724 (2022).
 - [62] O. Gühne and G. Tóth, Entanglement detection, *Phys. Rep.* **474**, 1 (2009).
 - [63] L.-M. Duan, G. Giedke, J. I. Cirac, and P. Zoller, Inseparability Criterion for Continuous Variable Systems, *Phys. Rev. Lett.* **84**, 2722 (2000).
 - [64] R. Simon, Peres-Horodecki Separability Criterion for Continuous Variable Systems, *Phys. Rev. Lett.* **84**, 2726 (2000).
 - [65] G. Vidal and R. F. Werner, Computable Measure of Entanglement, *Phys. Rev. A* **65**, 032314 (2002).
 - [66] M. B. Plenio, Logarithmic Negativity: A Full Entanglement Monotone That is not Convex, *Phys. Rev. Lett.* **95**, 090503 (2005).
 - [67] R. Horodecki, P. Horodecki, M. Horodecki, and K. Horodecki, Quantum entanglement, *Rev. Mod. Phys.* **81**, 865 (2009).
 - [68] J. D. Plumhof, T. Stöferle, L. Mai, U. Scherf, and R. F. Mahrt, Room-Temperature Bose-Einstein Condensation of Cavity Exciton-Polaritons in a Polymer, *Nat. Mater.* **13**, 247 (2014).
 - [69] G. Lerario, A. Fieramosca, F. Barachati, D. Ballarini, K. S. Daskalakis, L. Dominici, M. D. Giorgi, S. A. Maier, G. Gigli, S. Kená-Cohen, and D. Sanvitto, Room-Temperature Superfluidity in a Polariton Condensate, *Nat. Phys.* **13**, 837 (2017).
 - [70] C. N. Cohen-Tannoudji and S. Reynaud, Dressed-Atom Description of Resonance Fluorescence and Absorption Spectra of a Multi-Level Atom in an Intense Laser Beam, *J. Phys. B.: At. Mol. Phys.* **10**, 345 (1977).

METHODS

Dynamics of the source

We describe resonance fluorescence as a two-level system (2LS) with natural frequency ω_σ driven by a laser with intensity Ω . Formally, this is described by the Hamiltonian (we take $\hbar = 1$ along the paper)

$$H_\sigma = \Delta \sigma^\dagger \sigma + \Omega(\sigma^\dagger + \sigma), \quad (2)$$

where $\Delta = (\omega_\sigma - \omega_L)$ is the detuning between the 2LS and the laser of frequency ω_L , and σ^\dagger (σ) is the creation (annihilation) operator of the 2LS, which follow the pseudo-spin

algebra. The dissipation of the system is taken into account through the master equation

$$\partial_t \rho = i[\rho, H_\sigma] + \frac{\gamma_\sigma}{2} \mathcal{L}_\sigma(\rho), \quad (3)$$

where H_σ is the Hamiltonian in Eq. (2) and $\mathcal{L}_\sigma(\rho) \equiv 2\sigma\rho\sigma^\dagger - \rho\sigma^\dagger\sigma - \sigma^\dagger\sigma\rho$. When the laser drives the 2LS with a large intensity, the system enters into the so-called *Mollow* regime,²¹ which is characterized by its emission spectrum in the shape of a triplet, with a central line flanked by a pair of symmetric peaks. An archetypal spectrum of a driven 2LS with $\Delta = 0$ is shown as a dashed line in Fig. 1(a). The origin of the three peaks has a natural explanation in the context of the “dressed atom” picture,⁷⁰ which relates each of the four possible transitions between consecutive energy manifolds [shown in the inset of panel (a)] to the emission peaks. Keeping the intensity of the excitation constant and taking the driving laser out of resonance from the 2LS, the triplet splits further and the satellite peaks become the dominant feature of the spectrum as the central peak loses its intensity. This is shown in solid lines in Fig. 1(a). The processes that yield the emission spectrum can be obtained through the diagonalization of the Liouvillian of the system.²⁵ Thus, rewriting Eq. (3) as $\partial_t \rho = -M\rho$, one can find the energy of the transitions as the imaginary part of the eigenvalues of the matrix M . Figure 1(c) shows in solid lines the three energy lines available for the emission of the 2LS driven out of resonance. For comparison, we also show in dashed lines the energies that unfold when the excitation is resonant [and which give rise to the spectrum shown in dashed lines in panel (a)]. The main distinction between these two cases is that in the detuned case the lines are always splitted, even in the limit when $\Omega/\gamma_\sigma \rightarrow 0$. In the opposite regime, when the intensity of the excitation dominates over the detuning, i.e., when $\Omega \gg \Delta$, the splitted lines coincide again. For intermediate intensities, the energy lines are approximately given by $\omega_\pm = \omega_L \pm \sqrt{4\Omega^2 + \Delta^2}$ (the exact expression that takes into account the dissipation is given in Ref.¹⁶). The energies ω_\pm are associated to the transitions $|\pm\rangle \rightarrow |\mp\rangle$ (shown in Fig. 1(c) in blue and red); namely, quantum jumps that change the quantum state of the 2LS. These types of transitions dominate the dynamics of the driven 2LS when $\Delta \gtrsim \Omega$ and, because they change the quantum state of the 2LS, the same transition cannot take place twice in a row. Instead, they take place one after the other and yield a scheme of photon heralding, as we showed in the results section.

Excitation with quantum light

The theory of cascaded systems^{58,59} allows us to describe the excitation of an optical target with the emission from our source. Thus, the master equation describing our system is upgraded to (cf. section I of the Supplemental Material for

details of the derivation)

$$\begin{aligned} \partial_t \rho = & i[\rho, H_\sigma + H_t] + \frac{\gamma_\sigma}{2} \mathcal{L}_\sigma(\rho) + \frac{\Gamma_1}{2} \mathcal{L}_{a_1}(\rho) + \frac{\Gamma_2}{2} \mathcal{L}_{a_2}(\rho) - \\ & - \sqrt{\gamma_\sigma \Gamma_1/2} \left\{ [a_1^\dagger, \sigma \rho] + [\rho \sigma^\dagger, a_1] \right\} - \\ & - \sqrt{\gamma_\sigma \Gamma_2/2} \left\{ [a_2^\dagger, \sigma \rho] + [\rho \sigma^\dagger, a_2] \right\}, \quad (4) \end{aligned}$$

where H_σ is the Hamiltonian in Eq. (2) and H_t is the Hamiltonian describing the internal degrees of freedom of the optical target. Note that the terms in the bottom two lines of Eq. (4) are responsible for the unidirectional coupling between the source of light and the optical targets. For the case of the detectors used to measure the photon correlations in the first part of the Article, we set $H_t = H_d$ with the latter defined as $H_d = (\omega_1 - \omega_L) a_1^\dagger a_1 + (\omega_2 - \omega_L) a_2^\dagger a_2$, which takes into account the free energy of the detectors, and we let $\Gamma_1 = \Gamma_2 = \Gamma$ to be the rate at which the detectors decay. The terms in the second line of Eq. (4) are responsible for the unidirectional coupling between the source of light and the detectors. Conversely, for the case of the excitation of polaritons, we use the convention $a_1 \rightarrow a$, $a_2 \rightarrow b$, and we replace H_t with the polariton Hamiltonian $H_p = (\omega_a - \omega_L) a^\dagger a + (\omega_b - \omega_L) b^\dagger b + g(a^\dagger b + b^\dagger a)$, where we take into account a photon with energy ω_a and an exciton with energy ω_b coupled with a strength g . Finally, we introduced $\Gamma_1 = \Gamma_a$ and $\Gamma_2 = \Gamma_b$, the decay rates of the photon and exciton modes of the polaritons.

DATA AVAILABILITY

The data that support the plots within this paper and other findings of this study are available from the corresponding Author upon reasonable request.

CODE AVAILABILITY

The various codes used for modelling the data are available from the corresponding Author upon reasonable request.

ACKNOWLEDGEMENTS

J.C.L.C. was supported by the Polish National Agency for Academic Exchange (NAWA) under project TULIP with number PPN/ULM/2020/1/00235 and from the Polish National Science Center (NCN) ‘‘Sonatina’’ project CARMEL with number 2021/40/C/ST2/00155. M.S. was supported by the European Union’s Horizon 2020 research and innovation programme under the Marie Skłodowska-Curie project ‘‘AppQInfo’’ No. 956071, the National Science Centre ‘‘Sonata Bis’’ project No. 2019/34/E/ST2/00273, and the QuantERA II Programme that has received funding from the European Union’s Horizon 2020 research and innovation programme under Grant Agreement No 101017733, project ‘‘PhoMemtor’’ No. 2021/03/Y/ST2/00177.

AUTHOR CONTRIBUTIONS

J.C.L.C. proposed the idea. J.C.L.C. and S.B.F. developed the theoretical formalism and the conceptual tools, and then implemented the theoretical methods and analysed the data. J.C.L.C. and M.S. contributed material, analysis tools and expertise. J.C.L.C. wrote the main paper, the Supplemental Material, and supervised the research. All authors discussed the results and its implications and commented on the manuscript.

COMPETING INTERESTS

The authors declare no competing interests.

Supplemental Material: Entanglement in Resonance Fluorescence

Juan Camilo López Carreño,^{1,*} Santiago Bermúdez Feijoo,² and Magdalena Stobińska³

¹*Institute of Theoretical Physics, University of Warsaw, ul. Pasteura 5, 02-093, Warsaw, Poland*

²*Departamento de Física, Universidad Nacional de Colombia,*

Ciudad Universitaria, K. 45 No. 26–85, Bogotá D.C., Colombia

³*Faculty of Mathematics, Informatics and Mechanics, University of Warsaw, ul. Banacha 2, 02-097 Warsaw, Poland*

(Dated: June 19, 2023)

I. MEASURING THE EMISSION: CASCADED FORMALISM

In the main text we have described the detection of the emission from a 2LS with a pair of physical detectors (i.e., observing light at a fixed frequency $\tilde{\omega}$ with a finite linewidth $\tilde{\Gamma}$ and, possibly, non-ideal efficiency ϵ) using the so-called “cascaded formalism”. In general, such a theory [1, 2] allows to use light with a non-trivial temporal structure to be used as the source of excitation of an arbitrary optical target. Physically, the cascaded formalism allows to describe the coupling the source and the target of the excitation unidirectionally, i.e., letting the source evolve independently of the degrees of freedom of the target. In practice, such a coupling is realised by counteracting a reciprocal coupling (which enters as a Hamiltonian into the description of the system) with a dissipative coupling (which is not reciprocal and is taken into account as a Lindblad term on the master equation). The interplay between these two couplings yields a negative interference that cancels completely the terms that bring back from the target to the source of the light.

In this section we provide the general master equation of a source of light observed by a single detector (which is the case most commonly used, and which is textbook material), but we also provide the generalization to multiple detectors.

A. A single detector

Consider the excitation of an optical target, to which we associate an annihilation operator a , by the emission of a quantum optical source, associated to another annihilation operator σ . Assuming that the source-target system is described with Hamiltonian H , and the source and target of the excitation have decay rate γ_σ and Γ , respectively, the master equation governing their dynamics is given by (we use $\hbar = 1$ along the text)

$$\partial_t \rho = i[\rho, H] + \frac{\gamma_\sigma}{2} \mathcal{L}_\sigma \rho + \frac{\Gamma}{2} \mathcal{L}_a \rho + \sqrt{\epsilon \alpha \gamma_\sigma \Gamma} \{[\sigma \rho, a^\dagger] + [a, \rho \sigma^\dagger]\}, \quad (\text{S1})$$

where $\mathcal{L}_c \rho = (2c\rho c^\dagger - \rho c^\dagger c - c^\dagger c \rho)$, α is a factor that guarantees that Eq. (S1) is physical, and ϵ is the detector efficiency (in the following, we let $\epsilon = 1$, although the non-ideal case can be recovered by re-scaling $\alpha \rightarrow \epsilon \alpha$). In particular, note that the master equation (S1) is *not* evidently written in the Lindblad form. However, one can define an operator

$$\mathcal{O}_1 = \sqrt{\chi_1 \gamma_\sigma} \sigma + \sqrt{\chi_2 \Gamma} a, \quad (\text{S2})$$

with $0 \leq \chi_1, \chi_2 \leq 1$, in such a way that we can write

$$\frac{1}{2} \mathcal{L}_{\mathcal{O}_1} \rho = \chi_1 \frac{\gamma_\sigma}{2} \mathcal{L}_\sigma \rho + \chi_2 \frac{\Gamma}{2} \mathcal{L}_a \rho + \frac{1}{2} \sqrt{\chi_1 \chi_2 \gamma_\sigma \Gamma} (2\sigma \rho a^\dagger + 2a \rho \sigma^\dagger - \sigma^\dagger a \rho - \rho \sigma^\dagger a - a^\dagger \sigma \rho - \rho a^\dagger \sigma). \quad (\text{S3})$$

The term inside the brackets in the rightmost term of Eq. (S3) can be rewritten as

$$2([\sigma \rho, a^\dagger] + [a, \rho \sigma^\dagger]) + [\rho, \sigma^\dagger a - a^\dagger \sigma], \quad (\text{S4})$$

which can be replaced back into Eq. (S3) to yield

$$\frac{1}{2} \mathcal{L}_{\mathcal{O}_1} \rho = \chi_1 \frac{\gamma_\sigma}{2} \mathcal{L}_\sigma \rho + \chi_2 \frac{\Gamma}{2} \mathcal{L}_a \rho + \sqrt{\chi_1 \chi_2 \gamma_\sigma \Gamma} \{[\sigma \rho, a^\dagger] + [a, \rho \sigma^\dagger]\} + \frac{1}{2} \sqrt{\chi_1 \chi_2 \gamma_\sigma \Gamma} [\rho, \sigma^\dagger a - a^\dagger \sigma]. \quad (\text{S5})$$

* juclopezca@gmail.com

Reorganising the terms adequately and introducing $\alpha \equiv \chi_1 \chi_2$, we find that the dissipative terms in the master equation (S1) are given by

$$\frac{\gamma_\sigma}{2} \mathcal{L}_\sigma \rho + \frac{\Gamma}{2} \mathcal{L}_a \rho + \sqrt{\alpha \gamma_\sigma \Gamma} \{ [\sigma \rho, a^\dagger] + [a, \rho \sigma^\dagger] \} = \frac{1}{2} \mathcal{L}_{\mathcal{O}_1} \rho + (1 - \chi_1) \frac{\gamma_\sigma}{2} \mathcal{L}_\sigma \rho + (1 - \chi_2) \frac{\Gamma}{2} \mathcal{L}_a \rho - \frac{1}{2} \sqrt{\alpha \gamma_\sigma \Gamma} [\rho, \sigma^\dagger a - a^\dagger \sigma], \quad (\text{S6})$$

which yields the following master equation

$$\partial_t \rho = i[\rho, H + iH'] + \frac{1}{2} \mathcal{L}_{\mathcal{O}_1} \rho + (1 - \chi_1) \frac{\gamma_\sigma}{2} \mathcal{L}_\sigma \rho + (1 - \chi_2) \frac{\Gamma}{2} \mathcal{L}_a \rho. \quad (\text{S7})$$

Here $H' = (1/2) \sqrt{\alpha \gamma_\sigma \Gamma} (\sigma^\dagger a - a^\dagger \sigma)$ is a bi-directional coupling between the source and the target of the emission. However, the Lindblad term associated to the operator \mathcal{O}_1 [defined eq. (S2)] provides the destructive interference that prevents a back-action from the target to the source of the excitation, thus letting the dynamics of the source completely independent from the dynamics of the target.

Therefore, the master equation (S7) describes the source-target system (this time, with an explicit term coupling between the two parties, H'), while we identify three dissipative processes, namely:

1. a dissipative coupling, associated to the operator \mathcal{O}_1 , that negatively interferes with the Hamiltonian coupling to let the source of the excitation to remain oblivious to the dynamics of the target,
2. the effective decay rate of the source at rate $(1 - \chi_1) \gamma_\sigma$, and
3. the effective decay rate of the target at rate $(1 - \chi_2) \Gamma$.

B. Multiple detectors

The generalization to multiple targets is required when one analyzes the emission of the source at two (or more) frequencies. In such a case, the dynamics of the entire systems is governed by a master equation similar to Eq. (S1), namely

$$\partial_t \rho = i[\rho, H] + \frac{\gamma_\sigma}{2} \mathcal{L}_\sigma \rho + \sum_n \frac{\Gamma_n}{2} \mathcal{L}_{a_n} \rho + \sum_n \sqrt{\alpha_n \gamma_\sigma \Gamma_n} \{ [\sigma \rho, a_n^\dagger] + [a_n, \rho \sigma^\dagger] \}, \quad (\text{S8})$$

where we have assumed that each of the optical targets is associated with a bosonic field, with its corresponding annihilation operator a_n and decay rate Γ_n . In analogy to the case of a single target shown in the previous section, we introduce a set of jump operators

$$\mathcal{O}_n = \sqrt{\lambda_n \gamma_\sigma} \sigma + \sqrt{(1 - \kappa_n) \Gamma_n} a_n, \quad (\text{S9})$$

with $0 \leq \lambda_n, \kappa_n \leq 1$.

Following the steps shown in Eqs. (S3) and (S4), we can show that the Lindblad terms associated to these jump operators can be expressed as

$$\begin{aligned} \sum_n \frac{1}{2} \mathcal{L}_{\mathcal{O}_n} \rho = & \frac{\gamma_\sigma}{2} \mathcal{L}_\sigma \rho \sum_n \lambda_n + \sum_n \frac{\Gamma_n}{2} \mathcal{L}_{a_n} \rho - \sum_n \frac{\kappa_n \Gamma_n}{2} \mathcal{L}_{a_n} \rho + \sum_n \sqrt{\lambda_n (1 - \kappa_n) \gamma_\sigma \Gamma_n} \{ [\sigma \rho, a_n^\dagger] + [a_n, \rho \sigma^\dagger] \} + \\ & + \frac{1}{2} \sum_n \sqrt{\lambda_n (1 - \kappa_n) \gamma_\sigma \Gamma_n} [\rho, a_n^\dagger \sigma - \sigma^\dagger a_n]. \end{aligned} \quad (\text{S10})$$

Adequately reorganizing the terms and letting $\alpha_n \equiv \lambda_n (1 - \kappa_n)$, we find that the master equation (S8) can be rewritten as

$$\partial_t \rho = i \left[\rho, H + i \sum_n H'_n \right] + \left(1 - \sum_n \lambda_n \right) \frac{\gamma_\sigma}{2} \mathcal{L}_\sigma \rho + \sum_n \frac{\kappa_n \Gamma_n}{2} \mathcal{L}_{a_n} \rho + \sum_n \frac{1}{2} \mathcal{L}_{\mathcal{O}_n}, \quad (\text{S11})$$

where we have introduced $H'_n \equiv (1/2) \sqrt{\lambda_n (1 - \kappa_n) \gamma_\sigma \Gamma_n} (a_n^\dagger \sigma - \sigma^\dagger a_n)$. Thus, the dynamics of a source of light exciting n optical targets can be decomposed into a Hamiltonian dynamic—governed by the Hamiltonian $H + i \sum_n H'_n$ —and three types of dissipative processes, namely

1. the dissipative coupling between the source and the target of the excitation (associated to the operators \mathcal{O}_n), which prevents the back-action from the latter to the former,

2. the effective decay rate of the source at rate $(1 - \sum_n \lambda_n)\gamma_\sigma$, and
3. the effective decay rate of the targets at rates $\kappa_n\Gamma_n$.

The master equation that we have used to observe entanglement from the Mollow triplet (cf. Eq. (3) of the main text) is a particular case of Eq. (S11) when $\alpha_1 = \alpha_2 = 1/2$; which can be obtained, e.g., by letting $\lambda_1 = \lambda_2 = 1/2$ and $\kappa_1 = \kappa_2 = 0$, which in physical terms corresponds to the optimization of both the dissipative coupling and the amount of light that each detector receives.

II. ENTANGLEMENT AND VIOLATION OF THE CAUCHY-SCHWARZ INEQUALITY

The Cauchy-Schwarz inequality (CSI) is a fundamental result of mathematical analysis, which states that the inner product between two vectors, \vec{u} and \vec{v} , cannot be larger than the product between the norms of each of the vectors, namely

$$|\langle \vec{u} | \vec{v} \rangle|^2 \leq \langle \vec{u} | \vec{u} \rangle \cdot \langle \vec{v} | \vec{v} \rangle, \quad (\text{S12})$$

where $\langle \cdot | \cdot \rangle$ indicates inner product. In the context of optics, the CSI applies to the intensities and correlations between fields, and Eq. (S12) becomes

$$|\langle I_1 I_2 \rangle|^2 \leq \langle I_1^2 \rangle \langle I_2^2 \rangle, \quad (\text{S13})$$

where I_1 and I_2 are the intensities of (fluctuating) fields, and $\langle \cdot \rangle$ indicates mean value. While classical states satisfy Eq. (S13), in quantum mechanics one can encounter states whose correlations are larger than those allowed by the CSI [3, 4]. Therefore,

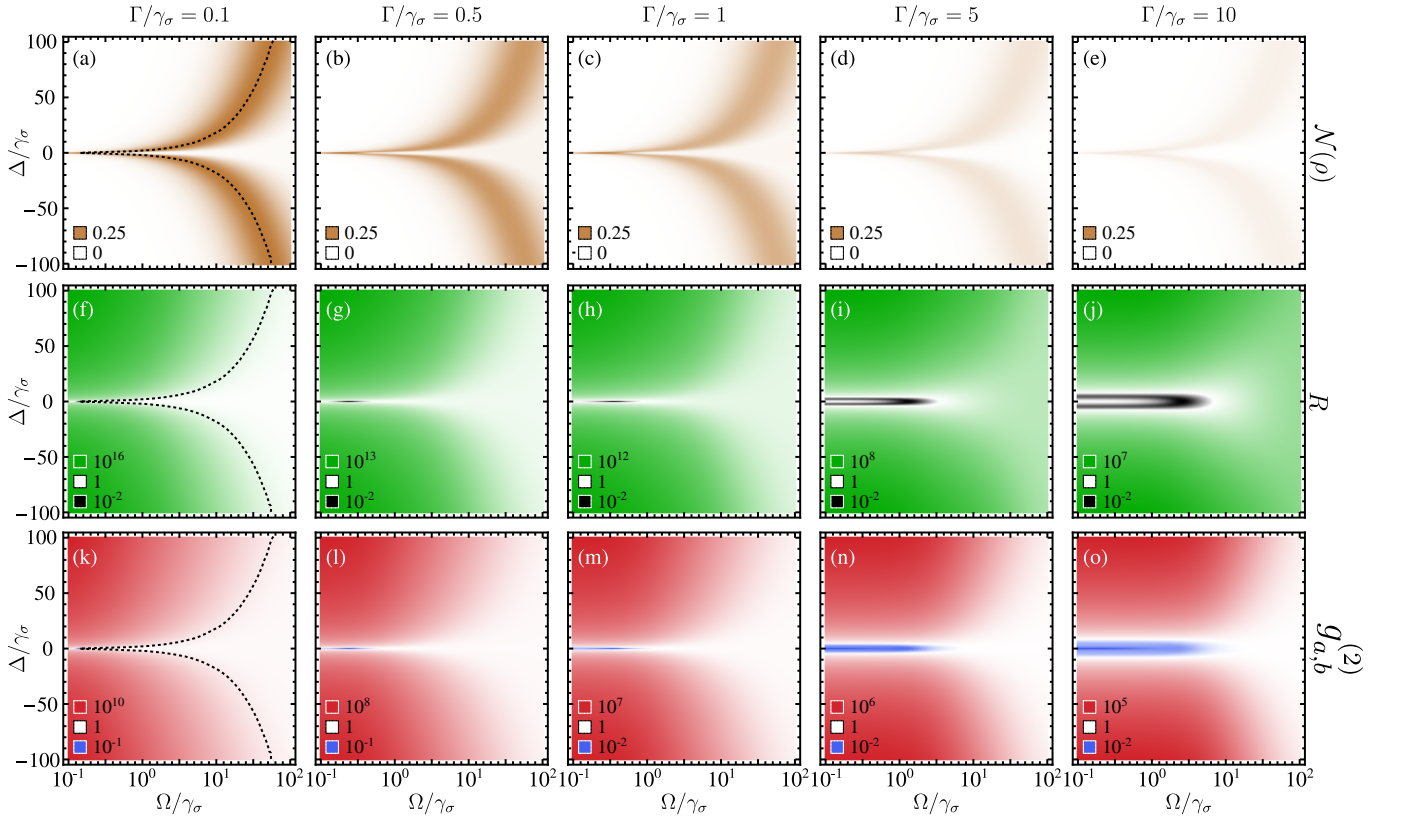


Figure 1. (Color online). Entanglement as shown through the logarithmic negativity (upper row), violation of the CSI (quantified through the R coefficient defined in Eq. (S15); middle row) and second-order correlation function (bottom row) between the photons emitted from the sidebands of the 2LS. All the figures are shown as a function of the detuning Δ between the 2LS and the driving laser and the intensity Ω with which the latter excited the former. From left to right, the columns display cases with an increasing linewidth of the detectors, showing, in particular, that entanglement is quickly lost as the linewidth of the detectors becomes larger than the linewidth of the 2LS, i.e., when $\Gamma \leq \gamma_\sigma$. On the column for $\Gamma/\gamma_\sigma = 0.1$ we indicate in dashed lines the parameters that provide the maximum entanglement that can be distilled from the 2LS. Notably, these parameters do not maximize the CSI violation nor the superbunching character of the photons. For broader values of Γ , the values of the maxima decrease, but they are located at the same parameters.

the violation of the CSI is used as an indicator of nonclassicality. In fact, the violation of the CSI has been recently linked with the appearance of entanglement [5, 6].

In the main text we deal with the entanglement between photons emitted from the lateral peaks of the Mollow triplet, namely with frequencies Ω_{\pm} . The observables of these photons are unveiled by letting them excite a pair of detectors, which have a finite linewidth, have natural frequencies that match the energy of the sidebands, and are described with annihilation operators a and b , both following Bose algebra. Thus, using the formalism of the second quantization, the inequality (S13) can be formulated in terms of the equal-time second-order correlation function of the operators of the detectors, namely

$$\left[G_{a,b}^{(2)}\right]^2 \leq G_{a,a}^{(2)}G_{b,b}^{(2)}, \quad (\text{S14})$$

where $G_{c,d}^{(2)} = \langle c^\dagger d^\dagger dc \rangle$ for $c, d \in \{a, b\}$. Thus, to quantify the degree of violation of the CSI, we introduce the coefficient

$$R = \frac{\left[G_{a,b}^{(2)}\right]^2}{G_{a,a}^{(2)}G_{b,b}^{(2)}}, \quad (\text{S15})$$

which is larger than one when the CSI is violated, i.e., when the state of the detectors is non-classical. Figure 1 shows the logarithmic negativity (top row), the degree of violation of the CSI (center row) and the second-order correlation function (bottom row) of the photons emitted from the sidebands of the Mollow triplet, as a function of both the intensity of the driving laser (Ω) and its detuning from the 2LS (Δ). The various columns corresponds to an increasing linewidth of the detectors Γ . We find that the three quantities are symmetric with respect to the detuning of the laser; namely, the behaviour of the emission is the same regardless of whether the laser is blue- or red-shifted from the 2LS. Analysing the figure, we observe that although the CSI is violated for a large range of parameters (cf. the green regions in the center row), the logarithmic negativity is only nonzero for a particular set of parameters. In fact, for $\Delta \gg \gamma_\sigma$ the driving intensity that optimises the entanglement is given by $\Omega \approx 0.58|\Delta|$, which is shown as a dashed line in panel 1(a). Notably, the parameters that provide the largest entanglement [as measured through $\mathcal{N}(\rho)$] do not correspond to a maximum in either the CSI violation nor the superbunching of the emitted photons. This means that, although the violation of classical inequalities is a requisite for entanglement, in our case, an increase in the nonlocality of the photon pair is not necessarily accompanied by an increase in the degree of their entanglement. Figure 2

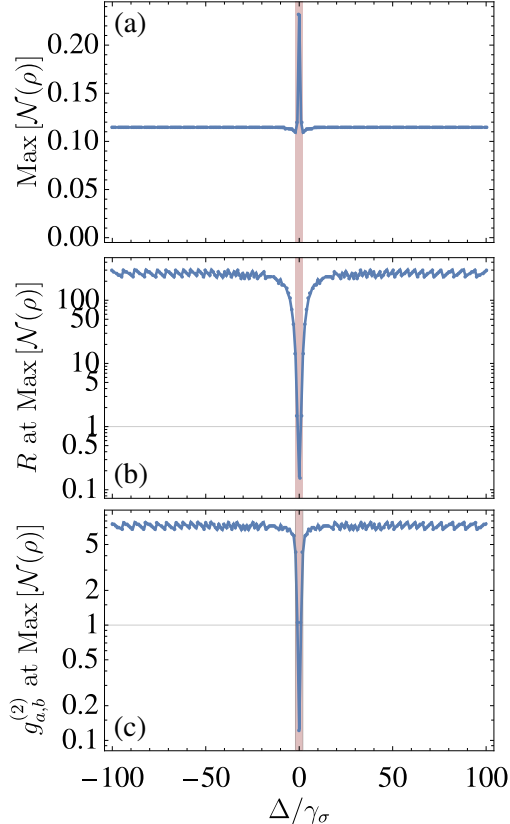


Figure 2. Optimized quantum correlations between photons emitted from the sidebands of a 2LS driven coherently with detuning Δ : (a) Maximum entanglement that can be distilled from the photons; (b) Degree of violation of the Cauchy-Schwarz inequality, as defined in Eq. (S15); and (c) Second-order correlation between the sidebands for the parameters that optimize the entanglement. In the region near resonance (when $\Delta \approx 0$, which we have highlighted in light red) we find a surge in the distillable entanglement. However, within such a region there coefficient R falls below 1, meaning that the state of the detectors is compatible with a classical state. Furthermore, in that same window the emission from the sidebands ceases to be heralded, as shown by their correlations becoming antibunched. Outside that region, however, the emitted photons violate the CSI inequality and are bunched. In fact, the three quantities quickly reach a value independent of the detuning between the 2LS and the driving laser.

shows the negativity, the R coefficient and the $g_{a,b}^{(2)}$ for the parameters that optimize the entanglement, i.e., for the dashed lines in the column with $\Gamma/\gamma_\sigma = 0.1$ in Fig. 1. We find that in the region where $\Omega_+ \leq \Gamma$ (which we have highlighted as a vertical red shade on the three panels) the negativity has a spike while the R coefficient drops below 1 and the cross-correlation between the sidebands becomes antibunched. Together, the three quantities suggest that in this regime the emission is not heralded (in fact, it is anticorrelated) and the state of the emitted photons is compatible with a classical state.

This is a consequence of the detection: when the linewidth of the detectors is large as compared to the size of the Mollow triplet, the detectors are collecting light from *all* the frequencies. In particular, they are observing photons emitted from other energy transitions, which are not strongly correlated with each others. Such a feature occurs when the linewidth of the detectors Γ is comparable to the splitting between the sidebands Ω_+ , which can take place in two distinct configurations. Firstly, when the triplet is well formed and the three peaks of the Mollow spectrum can be resolved (i.e., when $\Delta \gg \gamma_\sigma$ and/or $\Omega \gg \gamma_\sigma$). In this case, for the detectors to be comparable to the splitting, it must also be the case that $\Gamma \gg \gamma_\sigma$, which implies that we lose the spectral resolution over the 2LS, and that the observed correlations are washed out [7]. Secondly, when the emission lines of the triplet are close together so that they cannot be resolved (i.e., when both $\Delta \lesssim \gamma_\sigma$ and $\Omega \lesssim \gamma_\sigma$) and Γ is of the order of magnitude of γ_σ . In this case, we retain the spectral resolution, but the observed photons are indistinguishable in frequency (thus, the state of light is compatible with a classical state) and their wavefunction becomes factorisable. In fact, in this configuration the CSI is either completely satisfied or saturated, and the emission of the observed photons is uncorrelated (cf. the regions where $\Delta/\gamma_\sigma \approx 0$ and $\Omega < \gamma_\sigma$ in the central and bottom rows of Fig. 1). Thus, the increase of the logarithmic negativity shown in Fig. 2(a) is artificial. It is obtained from the detectors competing for the photons from both sidebands, and therefore it is describing “entanglement” of a light mode with itself, which does not have applications in quantum technologies. However, beyond the highlighted region in Fig. 2, provided that $\Omega_+ > \Gamma$, the three quantities reach a constant value that depends only on the ratio Γ/γ_σ ; namely, one can always find the intensity of the laser Ω and its detuning from the 2LS Δ , that yield the maximum possible entanglement. Furthermore, by comparing all the columns of Fig. 1, we find that while the optimal relation between intensity and detuning is independent of the linewidth of the detectors, an increase of this parameter only decreases the amount of distillable entanglement.

III. CONCURRENCE FROM POLARITONS

In the main text we introduced exciton-polaritons (henceforth, simply polaritons) as the strong coupling between a photon and an exciton. Assigning bosonic annihilation operators a and b to these modes, respectively, the polariton Hamiltonian becomes

$$H_p = (\omega_a - \omega_L)a^\dagger a + (\omega_b - \omega_L)b^\dagger b + g(a^\dagger b + b^\dagger a), \quad (\text{S16})$$

which describes a photon with energy ω_a and an exciton with energy ω_b coupled with a strength g . In the strong coupling regime, the energy levels of Hamiltonian (S16) hybridize, and the luminescence of the system takes place at the frequencies of the so-called *dressed states* of the system. Commonly, these states are known as the upper- and lower-polariton branches, and they are formally described with annihilation operators u and l , respectively. The latter two are related to the operators of the photon and of the exciton in the following way

$$l = \frac{1}{\sqrt{2}} \left(1 + \frac{\delta}{\sqrt{\delta^2 + 4g^2}} \right)^{1/2} a - \frac{1}{\sqrt{2}} \left(1 - \frac{\delta}{\sqrt{\delta^2 + 4g^2}} \right)^{1/2} b, \quad (\text{S17a})$$

$$u = \frac{1}{\sqrt{2}} \left(1 - \frac{\delta}{\sqrt{\delta^2 + 4g^2}} \right)^{1/2} a + \frac{1}{\sqrt{2}} \left(1 + \frac{\delta}{\sqrt{\delta^2 + 4g^2}} \right)^{1/2} b, \quad (\text{S17b})$$

where we have introduced the notation $\delta = \omega_b - \omega_a$. Using the transformation in Eq. (S17) the Hamiltonian (S16) becomes $H_p = (\omega_l - \omega_L)l^\dagger l + (\omega_u - \omega_L)u^\dagger u$, with the energies of the polariton branches defined as

$$\omega_l = \frac{1}{2} \left(\omega_a + \omega_b - \sqrt{\delta^2 + 4g^2} \right) \quad \text{and} \quad \omega_u = \frac{1}{2} \left(\omega_a + \omega_b + \sqrt{\delta^2 + 4g^2} \right). \quad (\text{S18})$$

Although polaritons are described as a bosonic field, when we excite them with the source of entangled photons described in the main text, we can safely assume that there are, at most, two excitations within the system. This means that one can limit the Hilbert space of the system and study the polariton entanglement by turning to a so-called *detection matrix* $\bar{\theta}$ [8]. The latter is constructed by from mean values of the density matrix ρ_{ss} obtained as a steady-state solution to the master equation (5) of the main text, namely

$$\bar{\theta} \equiv \frac{1}{\mathcal{N}} \begin{pmatrix} \langle\langle 0, 0 | \rho_{ss} | 0, 0 \rangle\rangle & \langle\langle 0, 0 | \rho_{ss} | 1, 0 \rangle\rangle & \langle\langle 0, 0 | \rho_{ss} | 0, 1 \rangle\rangle & \langle\langle 0, 0 | \rho_{ss} | 1, 1 \rangle\rangle \\ h.c. & \langle\langle 1, 0 | \rho_{ss} | 1, 0 \rangle\rangle & \langle\langle 1, 0 | \rho_{ss} | 0, 1 \rangle\rangle & \langle\langle 1, 0 | \rho_{ss} | 1, 1 \rangle\rangle \\ h.c. & h.c. & \langle\langle 0, 1 | \rho_{ss} | 0, 1 \rangle\rangle & \langle\langle 0, 1 | \rho_{ss} | 1, 1 \rangle\rangle \\ h.c. & h.c. & h.c. & \langle\langle 1, 1 | \rho_{ss} | 1, 1 \rangle\rangle \end{pmatrix}, \quad (\text{S19})$$

where we have introduced the notation $\lvert\lvert m, n \rangle\rangle$ to indicate a quantum state with m polaritons in the lower branch and n in the upper one. In the definition of the detection matrix we have included the normalization constant \mathcal{N} which guarantees that $\text{Tr}(\tilde{\theta}) = 1$, and $h.c.$ indicates the hermitian conjugate of the matrix element. Then, from the matrix in Eq. (S19) we obtain the concurrence as $C(\tilde{\theta}) \equiv \max(0, \lambda_1 - \lambda_2 - \lambda_3 - \lambda_4)$ where the λ_i are the eigenvalues in decreasing order of the matrix $\sqrt{\sqrt{\tilde{\theta}}\tilde{\theta}\sqrt{\tilde{\theta}}}$, where $\tilde{\theta} \equiv (\sigma_y \otimes \sigma_y)\tilde{\theta}^T(\sigma_y \otimes \sigma_y)$, and σ_y is a Pauli spin matrix.

-
- [1] C. W. Gardiner, Driving a Quantum System with the Output Field from Another Driven Quantum System, *Phys. Rev. Lett.* **70**, 2269 (1993).
 - [2] H. J. Carmichael, Quantum Trajectory Theory for Cascaded Open Systems, *Phys. Rev. Lett.* **70**, 2273 (1993).
 - [3] R. J. Glauber, The Quantum Theory of Optical Coherence, *Phys. Rev.* **130**, 2529 (1963).
 - [4] M. D. Reid and D. F. Walls, Violations of Classical Inequalities in Quantum Optics, *Phys. Rev. A* **34**, 1260 (1986).
 - [5] K. V. Kheruntsyan, J.-C. Jaskula, P. Deuar, M. Bonneau, G. B. Partridge, J. Ruaudel, R. Lopes, D. Boiron, and C. I. Westbrook, Violation of the Cauchy–Schwarz Inequality with Matter Waves, *Phys. Rev. Lett.* **108**, 260401 (2012).
 - [6] T. Wasak, P. Szańkowski, P. Ziń, M. Trippenbach, and J. Chwedeńczuk, Cauchy-Schwarz inequality and particle entanglement, *Phys. Rev. A* **90**, 033616 (2014).
 - [7] A. González-Tudela, F. P. Laussy, C. Tejedor, M. J. Hartmann, and E. del Valle, Two-Photon Spectra of Quantum Emitters, *New J. Phys.* **15**, 033036 (2013).
 - [8] Á. Cuevas, J. C. López Carreño, B. Silva, M. D. Giorgi, D. G. Suárez-Forero, C. Sánchez Muñoz, A. Fieramosca, F. Cardano, L. Marrucci, V. Tasco, G. Biasiol, E. del Valle, L. Dominici, D. Ballarini, G. Gigli, P. Mataloni, F. P. Laussy, F. Sciarrino, and D. Sanvitto, First Observation of the Quantized Exciton-Polariton Field and Effect of Interactions on a Single Polariton, *Sci. Adv.* **4**, eaao6814 (2018).